HEAT LOAD PREDICTION IN DISTRICT HEATING AND COOLING SYSTEMS THROUGH A RECURRENT NEURAL NETWORK WITH DATA CHARACTERISTICS

M. Sakawa, H. Katagiri, T. Matsui, K. Ishimaru and S. Ushiro

Received August 20, 2010; revised September 5, 2010

Abstract. Heat load prediction in district heating and cooling (DHC) systems is one of the key technologies for economical and safe operations of DHC systems. The heat load prediction method using a three-layered neural network proposed by the authors has been used in an actual DHC plant on a trial basis. However, there exists a drawback that its prediction becomes less accurate in periods when the heat load is nonstationary. In this paper, we improve the heat load prediction method through the introduction of a recurrent neural network for adapting the dynamical variation of heat load together with a new kind of input data in consideration of the characteristics of heat load data. In order to show the efficiency of the proposed method, we carry out several numerical experiments using actual heat load data.

1 Introduction Recently, in urban areas, district heating and cooling (DHC) systems which aim at saving energy, saving space and preventing air-pollution, have been introduced actively. To be more specific, a DHC plant intensively makes cold water, hot water and steam used mainly for air conditioning and supplies them to all facilities in a certain district. Since there exist a number of large-size freezers and boilers in a DHC plant, it is possible to optimize the operation plan of these instruments if we can predict the heat load for the DHC plant with high accuracy in advance.

Unfortunately, in general, measurement noises, outliers and missing data are involved in actual heat load data used for prediction. For the purpose of removing such noise components from time series data, many techniques have been proposed until now. The Kalman filter [3] is one of most well-known filters. However, since the Kalman filter was designed to remove measurement noises, it may be inefficient for removing outliers or missing data. Martin and Thompson [4] proposed a new filtering algorithm, called robust filter, as an extension of the Kalman filter, for predicting time series involving not only measurement noises but also outliers or missing data. Moreover, the extension of the robust filter [4] to a nonlinear state space model was proposed by Connor and Martin [1]. They proposed a time series prediction method by a recurrent nonlinear auto regressive moving average (NARMA) model, which is a combination of a robust filter and an NARMA model using a recurrent neural network. With respect to heat load prediction of DHC systems, Dotzauer [2] proposed a prediction method based on linear regression and Sakawa et al. [9, 10] proposed a simplified robust filter and constructed a new prediction method based on an RBF-NARMA model which is an NARMA model through a radial basis function network (RBFN) since it is reported that the Kalman filter and robust filters have a shortcoming in the stability of complicated matrix calculations. In their prediction method, the network used for prediction has only one output unit. Since their method has a defect that the

2000 *Mathematics Subject Classification.* Primary 65F10, 65F15; Secondary 65H10, 65F03.

Key words and phrases. District heating and cooling system, heat load prediction, recurrent neural network, data characteristics .

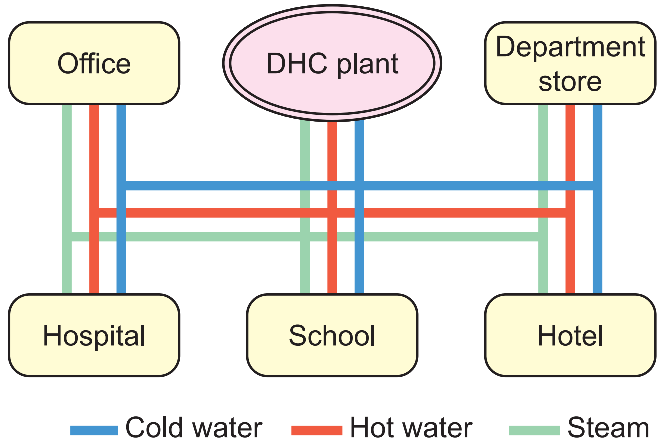

Figure 1: A district heating and cooling (DHC) system.

accuracy of prediction becomes low at a steep part of heat load data, Sakawa et al. [7] proposed a new prediction method based on the simplified robust filter and a three-layered neural network (TLNN) with multiple output units and showed its superiority to previous methods [9, 10]. The TLNN-based prediction method proposed in [7] is used in an actual DHC plant on trial. Its accuracy of prediction is sufficiently good in practical use for the period when the heat load is stationary but it becomes worse for the period when the heat load is nonstationary.

Under these circumstances, in this paper, we attempt to improve the heat load prediction method for DHC systems by incorporating a recurrent neural network for adapting the dynamical variation of heat load and new input data in consideration of the characteristics of heat load data as countermeasures for the deterioration of prediction accuracy in nonstationary periods.

2 District heating and cooling system It has been more and more important to introduce district heating and cooling (DHC) systems into urban areas as the need for the environmental preservation and the efficient use of energy becomes higher and higher. By the introduction of DHC systems, we can expect various advantages like saving energy, saving space, preventing air-pollution and so forth. In a DHC system, a DHC plant intensively makes cold water, hot water and steam used mainly for air conditioning and supplies them to all facilities in a certain district. The overview of a DHC system is shown in Fig. 1.

Since there exist many large-size heat source instruments like boilers and freezers in a DHC plant, it is economically desirable to determine the optimal operation plan of them in consideration of predicted values of heat load and the warm-up time of each instrument [5, 6, 8]. In particular, for a DHC plant with a thermal storage system using midnight electricity, a more efficient and less redundant operation plan can be realized if we can accurately predict future heat load. Thus, the heat load prediction is indispensable for the efficient operation of a DHC system. From this viewpoint, the authors have developed several heat load prediction methods for DHC systems [9, 10, 7] and have shown the superiority of one using a three-layered neural network (TLNN). The TLNN-based prediction method proposed in [7] is tentatively used in an actual DHC plant. It is reported that it can predict heat load with high accuracy in periods when heat load is stationary while the accuracy of prediction becomes low in periods when heat load is nonstationary. Here, the term “stationary” means

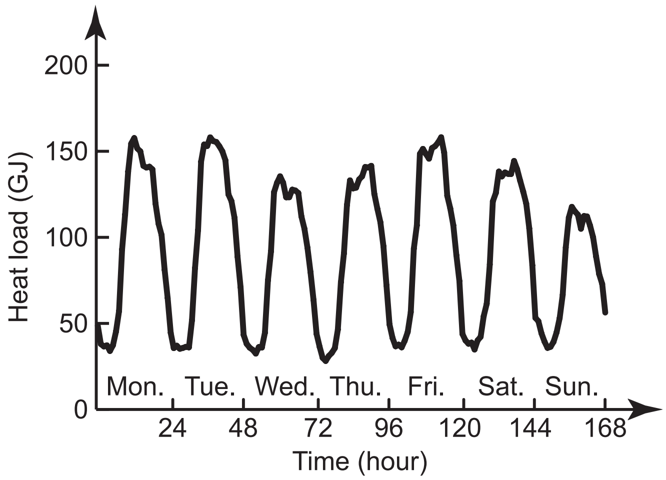

Figure 2: Heat load data of a week.

that the average heat load in a day seems to keep almost the same value day by day during a certain period. Otherwise, i.e., when the average heat load in a day seems to significantly vary according to seasonal factors (trend, seesaw, etc.), we use the term "nonstationary".

In the present paper, for the purpose of improving the accuracy of heat load prediction, we add a new input data for heat load prediction and adopt a recurrent neural network as the prediction network to capture the dynamical variation of heat load by reconsidering characteristics of heat load data.

3 Characteristic of heat load data in DHC systems

3.1 Outline of heat load data When we consider the heat load prediction in DHC systems, it is important to understand characteristics of heat load data. Figure 2 shows an actual heat load data for a week, which is sampled by one hour.

From this figure, the characteristics of heat load data can be summarized as:

(1) The heat load increases sharply around 9:00 (the opening hours of offices), then, keeps high level till the evening. It decreases gradually after the closing hours of offices, and indicates almost zero at late hours. As a result, it has a circadian cycle.

(2) There is the one-week cycle such that maximal values of heat load data on weekends (Saturday and Sunday) are smaller than those on weekdays (from Monday to Friday). However, exceptionally, maximal values on national holidays also becomes as small as on weekends.

3.2 Relationship between average heat load and open-air temperature Figure 3 shows the relationship between the highest open-air temperature in a day and the average heat load in a day. From this figure, we recognize that there exists the close relationship between the average heat load in a day and the highest open-air temperature in a day, i.e., the average heat load increases as the highest open-air temperature becomes high.

In consideration of the characteristics of heat load data, the last 24-hour heat load, the day of the week and the (predicted) highest open-air temperature in a day are used as explanatory variables of heat load in past researches [9, 10, 7].

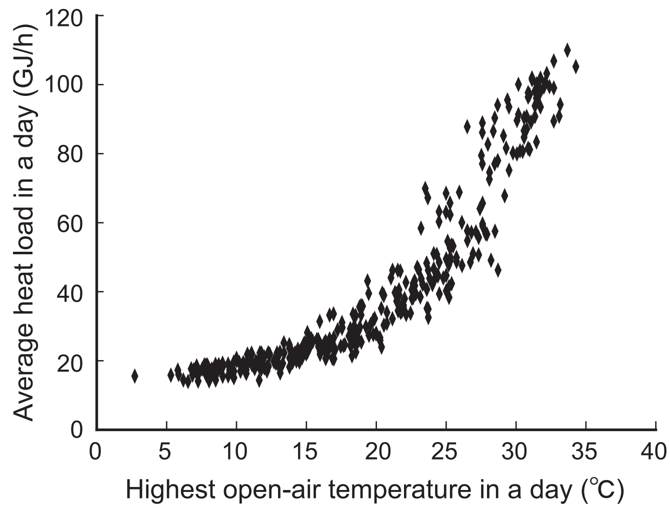

Figure 3: The relationship between the highest open-air temperature in a day and the average heat load in day.

Table 1: CR and AIC for the average heat load in a day.

Explanatory variables for heat load	CR	AIC
The heat load in the previous day & the highest open-air temperature in a day	0.817	1761.17
The heat load in the previous day & the highest open-air temperature in a day & the lowest open-air temperature in a day	0.849	1693.48

Figure 4 illustrates the transition of the heat load in an hour, the highest open-air temperature in a day and the lowest open-air temperature in a day in some period.

From this figure, we understand that heat load tends to be large if the highest open-air temperature in a day is high in general. On the other hand, the heat load in the seventh day are as high as those in the previous day in spite of the decline of the highest open-air temperature. This fact indicates that there should exist some factor to affect heat load aside from the highest open-air temperature in a day. It should be noted that the lowest open-air temperature in the seventh day is almost the same as that in the previous day. For example, in cloudy or rainy days in summer, such a situation often occurs and we are likely to use air conditioners in those days as strongly as in a fine day since the humidity becomes higher. From this case, we suppose that the lowest open-air temperature in a day should affect heat load.

In the following, we investigate the effect of the lowest open-air temperature in a day on heat load prediction. Table 1 shows the contribution ratio (CR) and Akaike's information criterion (AIC) when we use the heat load in the previous day and the highest open-air temperature in a day as explanatory variables for the average heat load in a day as well as those when we use the heat load in the previous day, the highest open-air temperature in a day and the lowest open-air temperature in a day as explanatory variables for the average heat load in a day. Since the improvement of CR and AIC suggests that the lowest open-air temperature in a day should significantly affect heat load, it is adopted as a new

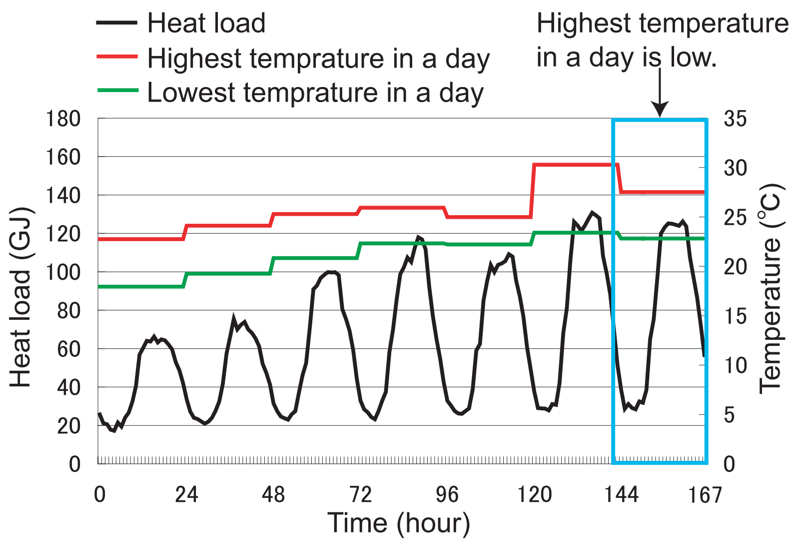

Figure 4: The transition of the heat load in an hour, the highest open-air temperature in a day and the lowest open-air temperature in a day.

explanatory variable for heat load in this paper.

4 Heat load prediction through neural network

4.1 An existing method of heat load prediction One of most practical existing methods for heat load prediction of DHC systems was proposed by Sakawa et al. [7]. In their method, a kind of layered neural networks with multiple output units was used, as shown in Fig. 5.

Let the present time be t. Using the observed heat load data set for 24 hours $\{y(t-23), y(t-22), \ldots, y(t)\}$, the day of the week of the predicted day $d_1, d_2, \ldots, d_7$ and the predicted highest open-air temperature of the predicted day $\hat{T}_{\max}$, the input data vector of the neural network shown in Fig. 5, $\boldsymbol{x} = (x_1, \ldots, x_{32})^T$, is represented as:

$$\boldsymbol{x} = (y(t-23), y(t-22), \ldots, y(t), d_1, d_2, \ldots, d_7, \hat{T}_{\max})^T.$$

Each element of the output vector $\boldsymbol{z} = (z_1, z_2, \ldots, z_{24})^T$ is the predicted heat load from $t+\alpha+1$ to $t+\alpha+24$. Figure 6 shows the relationship between the input (learning) heat load data and the output (predicted) one.

In this paper, we adopt the following sigmoid function

$$S(x) = \frac{1}{1+\exp(-x)}$$

as the output function of each element in the hidden layer and the output layer. Then, the output vector $\boldsymbol{z} = (z_1, z_2, \ldots, z_{24})^T$ is expressed as:

$$z_k = S\left(\sum_{j=1}^{q} w_{kj} g_j + \eta_k\right), \quad k = 1, 2, \ldots, 24, \tag{1}$$

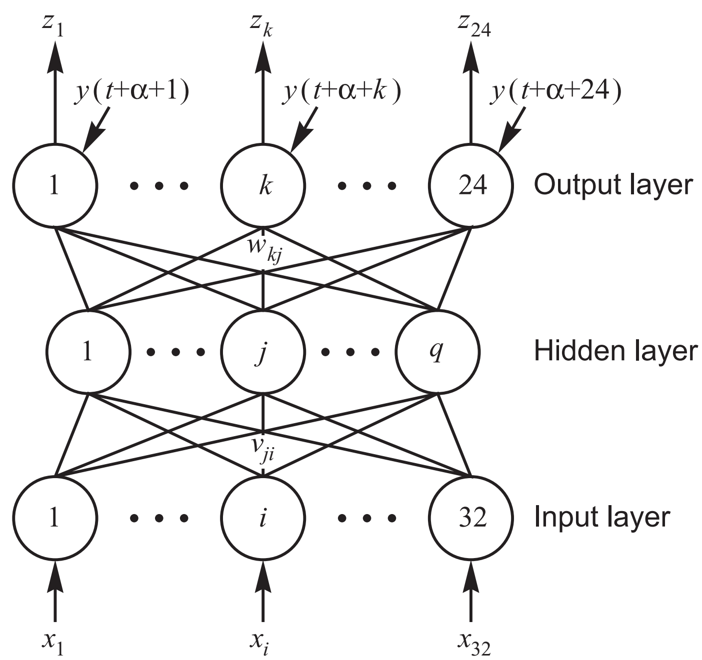

Figure 5: A three-layered neural network with 32 input units and 24 output ones.

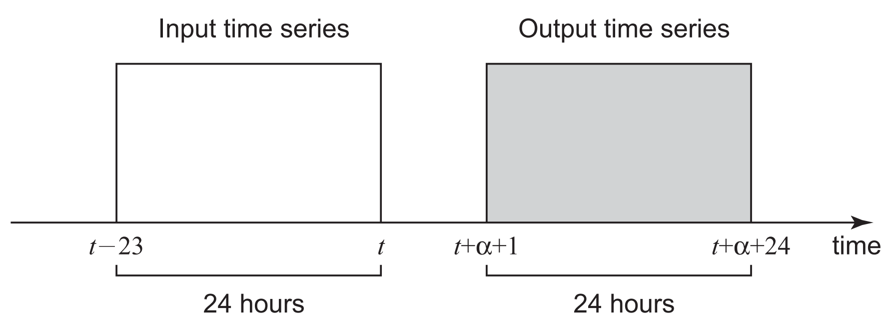

Figure 6: The relationship between the input (learned) heat load data and the output (predicted) one.

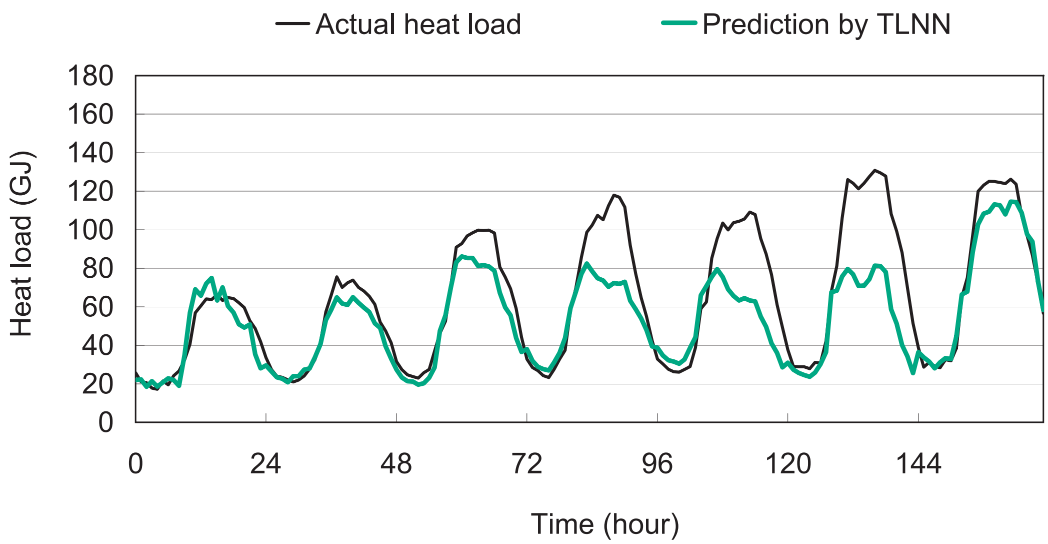

Figure 7: Heat load prediction by TLNN [7] for the nonstationary period.

where η_k is the threshold of the k th unit of the output layer. In (1), g_j is the output of the j th unit of the hidden layer calculated as:

$$g_j = S\left(\sum_{i=1}^{32} v_{ji} x_i + \theta_j\right), \quad j = 1, 2, \ldots, q,$$

where θ_j is the threshold of the j th unit of the hidden layer. Furthermore, we denote the teacher data by $\boldsymbol{y} = (y(t+\alpha+1), \ldots, y(t+\alpha+24))^T$.

Weights of the network, w_{kj} and v_{ji}, are determined to minimize the mean square error between the network output vector $\boldsymbol{z}$ and the teacher data vector $\boldsymbol{y}$ defined as:

$$E = \frac{1}{2P} \sum_{p=1}^{P} ||\boldsymbol{z}^p - \boldsymbol{y}^p||^2 \tag{2}$$

by the learning based on the error back propagation method [11]. In (2), P is the number of learning data patterns.

By now, the three-layered neural network (TLNN) proposed by Sakawa et al. [7] has showed better performance than previous methods [9, 10] and it is tentatively used in an actual DHC plant. In the practical use of the TLNN-based method [7], it is reported that its accuracy of prediction is sufficiently good for the period when the heat load is stationary but it becomes worse for the period when the heat load is nonstationary, for example, it involves trend as illustrated in Fig. 7. As a reason of this deterioration of prediction, it is considered that the layered network is not good at reading the trend of heat load from the heat load data for 24 hours given as input data.

4.2 Heat load prediction considering the characteristic of heat load In consideration of shortcomings of the TLNN-based prediction method [7], in this paper, we adopt a neural network of recurrent type to capture the nonstationary change of heat load and use the predicted lowest open-air temperature of the predicted day as a new input data.

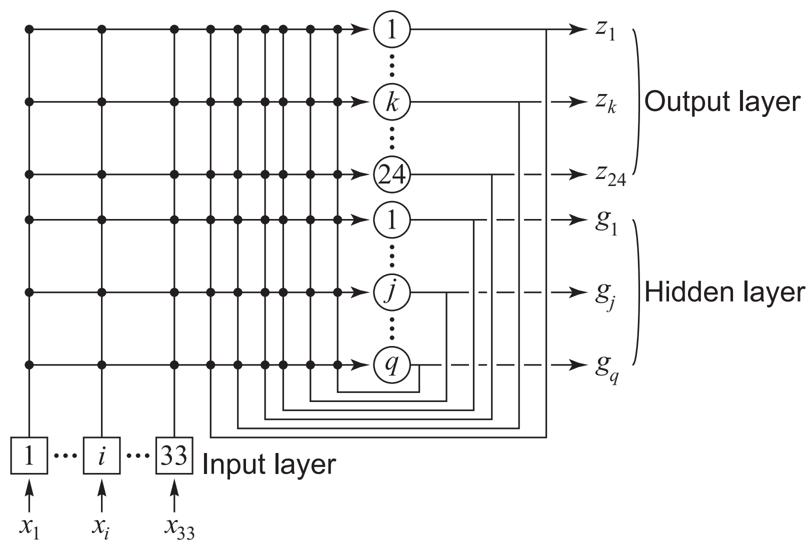

Figure 8: Recurrent neural network with 33 input units and 24 output ones.

To be more specific, in a new prediction method proposed in this paper, we adopt a recurrent neural network with 33 input units and 24 output ones as shown in Fig. 8. It is difficult for the layered neural network mentioned in the previous section to capture the trend of heat load because it uses heat load data for only one day as the input. On the other hand, the recurrent neural network is expected to capture the trend of heat load since it can save and utilize the information of heat load data before the previous day.

Using the observed heat load at each time $y(\cdot)$, the day of the week of the predicted day $d_1, d_2, \ldots, d_7$, the predicted highest open-air temperature of the predicted day $\hat{T}_{\max}$ and the predicted lowest open-air temperature of the predicted day $\hat{T}_{\min}$, the input data of the recurrent neural network at discrete step τ, $\boldsymbol{x}(\tau) = (x_1(\tau), x_2(\tau), \ldots, x_{33}(\tau))^T$, is represented as:

$$\boldsymbol{x}(\tau) = (y(t_\tau - 23), \ldots, y(t_\tau), d_1, \ldots, d_7, \hat{T}_{\max}, \hat{T}_{\min})^T.$$

Let us denote the index set of input units, that of hidden units and that of output units by I, H and O, respectively. Furthermore, assume that the output function of each hidden unit is the sigmoid function defined as:

$$S(x) = \frac{1}{1 + \exp(-x)}$$

as well as that of each output unit.

Then, the output of the j th hidden unit at step $\tau + 1$ $g_j(\tau + 1)$, $j \in H$, is expressed as:

$$g_j(\tau + 1) = S\left(\sum_{i \in I} w_{ji} x_i(\tau) + \sum_{l \in H} w_{jl} g_l(\tau) + \sum_{k \in O} w_{jk} z_k(\tau) + \theta_j\right), \ j \in H,$$

and the output of the k th output unit at step $\tau + 1$ is expressed as:

$$z_k(\tau + 1) = S\left(\sum_{i \in I} w_{ki} x_i(\tau) + \sum_{j \in H} w_{kj} g_j(\tau) + \sum_{l \in O} w_{kl} z_l(\tau) + \eta_k\right), \ k \in O.$$

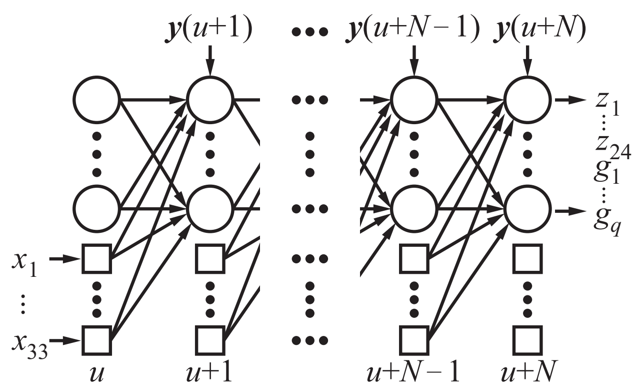

Figure 9: Epochwise error back propagation through time

4.3 Learning method of the recurrent neural network In this paper, we adopt the epochwise back propagation through time (EBPTT) proposed by Williams and Zipser [12] as the extension of back propagation learning [11] for the recurrent neural network in Fig. 8. In the EBPTT method, input data $\boldsymbol{x}(u), \boldsymbol{x}(u+1), \ldots, \boldsymbol{x}(u+N-1)$ at step $\tau = u, u+1, \ldots, u+N-1$ and teacher data $\boldsymbol{y}(u+1), \ldots, \boldsymbol{y}(u+N-1), \boldsymbol{y}(u+N)$ at step $\tau = u+1, \ldots, u+N-1, u+N$ are given to the recurrent neural network as shown in Fig. 9. Then, the total error function of the network is defined as:

$$J(u, u+N) = \frac{1}{2} \sum_{\tau=u+1}^{u+N} \sum_{k \in O} (z_k(\tau) - y_k(\tau))^2. \tag{3}$$

For the purpose of obtaining weights of the network w_{ij} to minimize the total error function, w_{ij} are updated as:

$$\Delta w_{ij} = -\eta \sum_{\tau=u}^{u+N-1} \delta_i(\tau+1) z_j(\tau), \tag{4}$$

$$w_{ij} = w_{ij} + \Delta w_{ij}. \tag{5}$$

In the above equation, $\delta_i(\tau)$, $u+1 \leq \tau \leq u+N-1$ are expressed as:

$$\delta_i(\tau) = y_i(\tau)\,(1 - y_i(\tau)) \cdot \left((y_i(\tau) - d_i(\tau)) + \sum_{l \in H \cup O} w_{li} \delta_l(\tau+1) \right), \tag{6}$$

while $\delta_i(\tau)$, $\tau = u+N$ is expressed as:

$$\delta_i(u+N) = (y_i(u+N) - d_i(u+N)) \cdot y_i(u+N) \cdot (1 - y_i(u+N)). \tag{7}$$

4.4 About filtering In past literatures [9, 10, 7], filtering techniques like a simplified robust filter have been used to deal with outliers and missing data in heat load data of DHC systems. In the present situation, however, there exist few outliers and missing data in heat load data because of the improvement of the data recording technique. Therefore, in this paper, we remove the filtering process from the prediction procedure for the reduction of processing time.

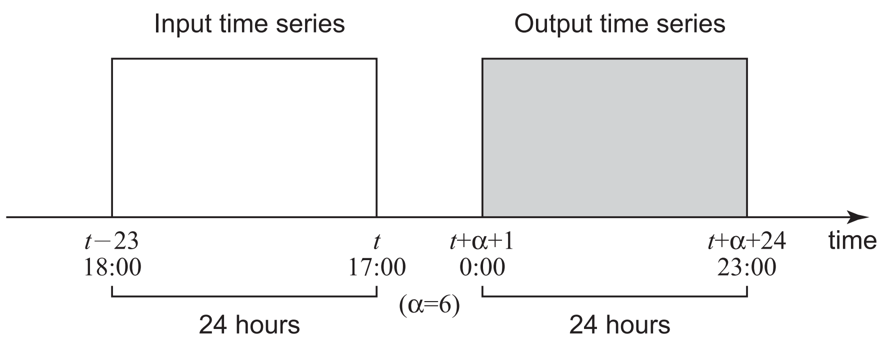

Figure 10: The relationship between the input heat load data and the output one for prediction networks.

Table 2: Results for a nonstationary period from 2002/07/01 to 2002/07/07.

	MSE (GJ^2)	PNRMSE (%)
TLNN [7]	21.05^2	25.93
TLNN with lowest	20.79^2	25.50
RNN (proposed)	11.82^2	14.56

5 Numerical experiments For the purpose of showing the efficiency of the proposed method through the recurrent neural network (RNN), we compare the result of heat load prediction by RNN with that of the best existing method by the three-layered neural network (TLNN) [7]. In the present paper, in order to predict heat load for 24 hours in one day (called "the predicted day"), we use heat load and temperature data of 28 days previous to the predicted day for learning.

In actual DHC systems, it is desired that heat load prediction is executed at the closing time (17:00) of the day previous to the predicted day (called "the previous day"). For this requirement, neural networks used in this paper are made to learn so that they predict heat load from 0:00 to 23:00 of the predicted day using heat load from 18:00 of the day just before the previous day to 17:00 of the previous day as input heat load data. Then, the relationship between the input heat load data and the output one for prediction networks is illustrated in Fig. 10.

In the following experiments, all computer programs are made by the authors and executed on a personal computer.

First, in order to investigate the effectiveness of incorporating the lowest open-air temperature and RNN, we apply TLNN using heat load data and highest open-air temperature data [7] (TLNN), TLNN using heat load data, highest open-air temperature data and lowest open-air temperature (TLNN with lowest) and RNN using heat load data, highest open-air temperature data and lowest open-air temperature (RNN) into heat load prediction in a period when heat load seems nonstationary, e.g., from 2002/07/01 to 2002/07/07.

Prediction results obtained by these three prediction methods are shown in Fig. 11, Fig. 12 and Fig. 13, respectively. Table 2 shows mean square errors (MSE) and percent normalized root mean square errors (PNRMSE).

In the period from 2002/07/01 to 2002/07/07, heat load has a slight increase trend, i.e., the average heat load increases day by day. It is observed that the predicted heat load by TLNN are considerably less than actual heat load. By incorporating the lowest

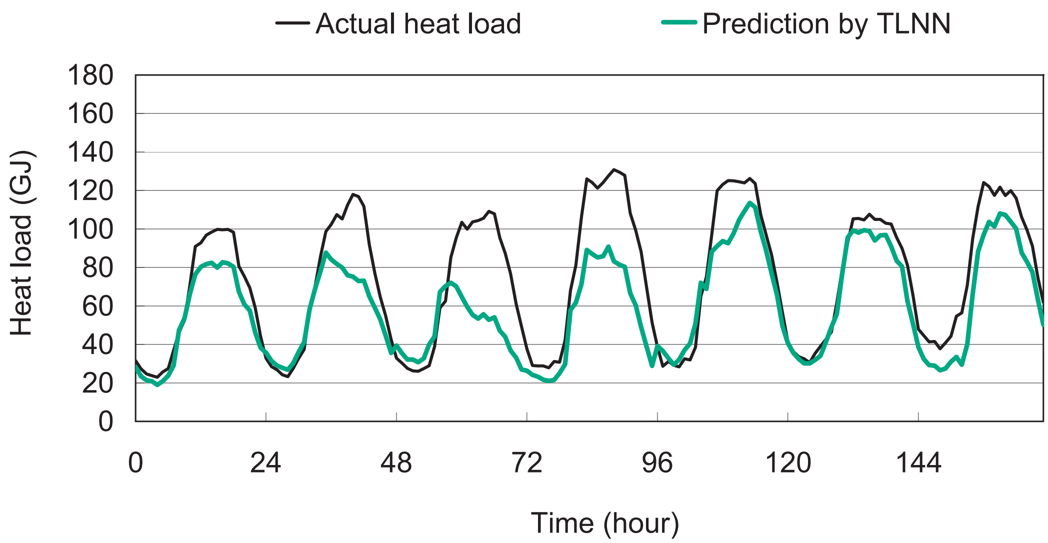

Figure 11: Prediction result by TLNN [7] for a nonstationary period from 2002/07/01 to 2002/07/07.

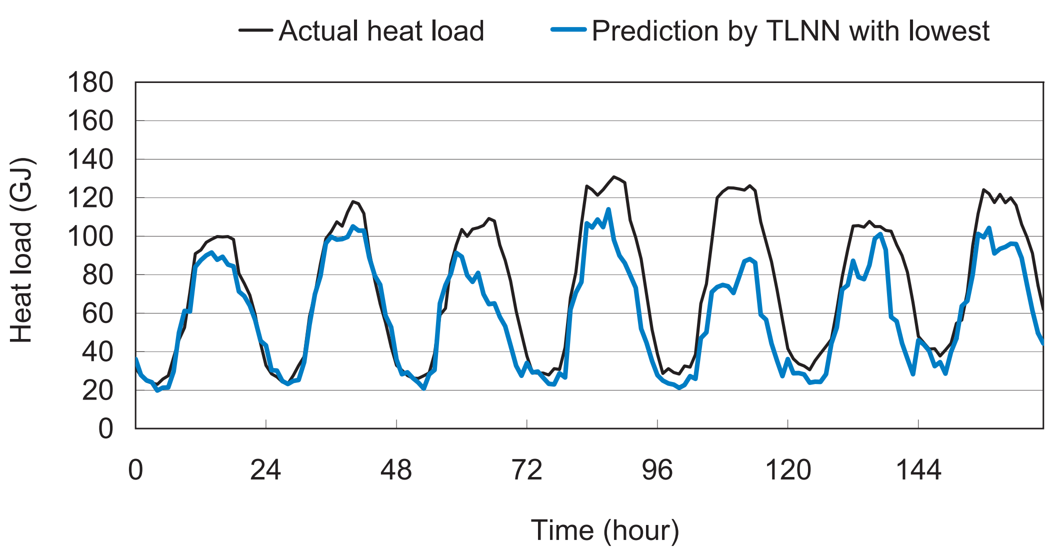

Figure 12: Prediction result by TLNN with the lowest open-air temperature for a nonstationary period from 2002/07/01 to 2002/07/07.

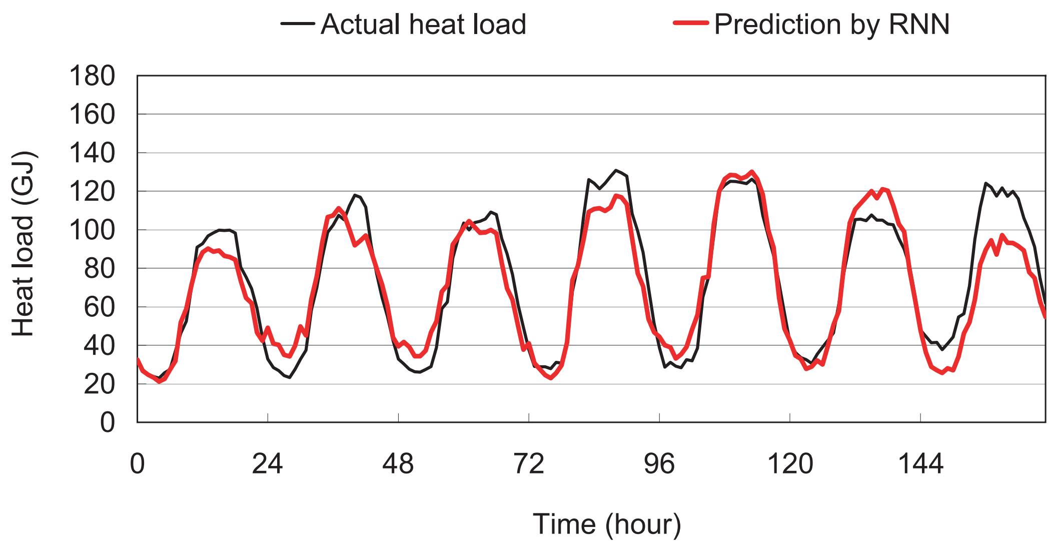

Figure 13: Prediction result by RNN for a nonstationary period from 2002/07/01 to 2002/07/07.

Table 3: Results for a stationary period from 2002/07/22 to 2002/07/28.

	MSE (GJ^2)	PNRMSE (%)
TLNN [7]	10.60^2	10.42
TLNN with lowest	9.30^2	9.14
RNN (proposed)	8.97^2	8.81

open-air temperature into TLNN (TLNN with lowest), we can obtain a little more accurate prediction than that by TLNN, but only the introduction of the lowest open-air temperature is not enough because the predicted values by TLNN with lowest are greatly different from the actual heat load, especially, around the peak position on each day.

On the other hand, it should be noted here that the proposed RNN can predict the peak values better than TLNN and TLNN with lowest since the proposed RNN using the lowest open-air temperature can capture the trend appropriately.

With respect to the average processing time, the proposed RNN takes 122.5 seconds while TLNN does 72.3 seconds. From the viewpoint of practical use, they will be sufficiently acceptable. The above experiment indicates that the performance of the proposed RNN is higher than those of TLNN and TLNN with lowest for a period when heat load is nonstationary.

Next, we investigate the performance of these three methods for a period when heat load seems stationary since stationary periods are seen more often than nonstationary periods. Here, we predict heat load by TLNN, TLNN with lowest and RNN for a stationary period, e.g., from 2002/07/22 to 2002/07/28.

Prediction results obtained by TLNN, TLNN with lowest and RNN are shown in Fig. 14, Fig. 15 and Fig. 16, respectively. Table 3 shows mean square errors (MSE) and percent normalized root mean square errors (PNRMSE).

For the stationary period as well as for the nonstationary one, TLNN with lowest can

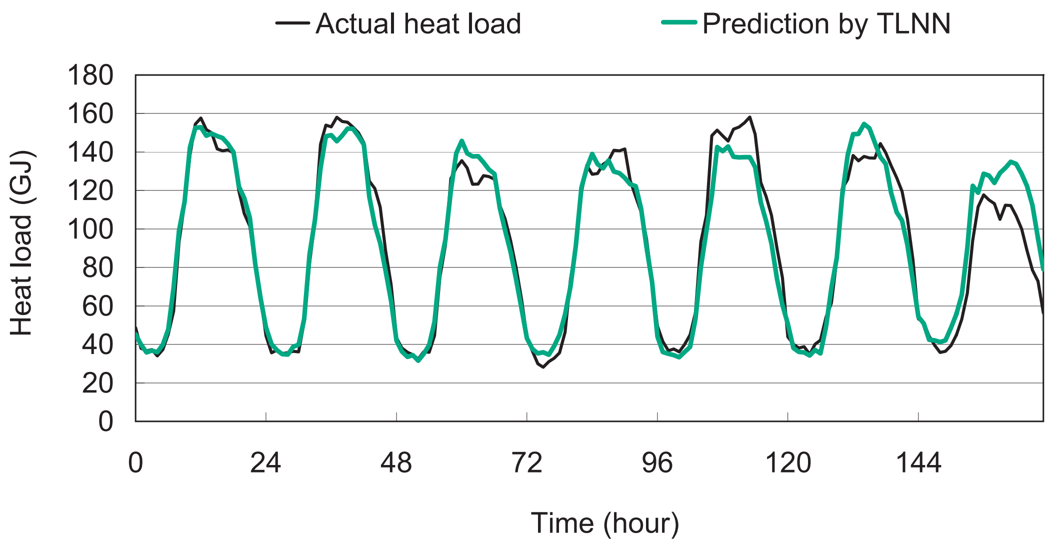

Figure 14: Prediction result by TLNN [7] for a stationary period from 2002/07/22 to 2002/07/28.

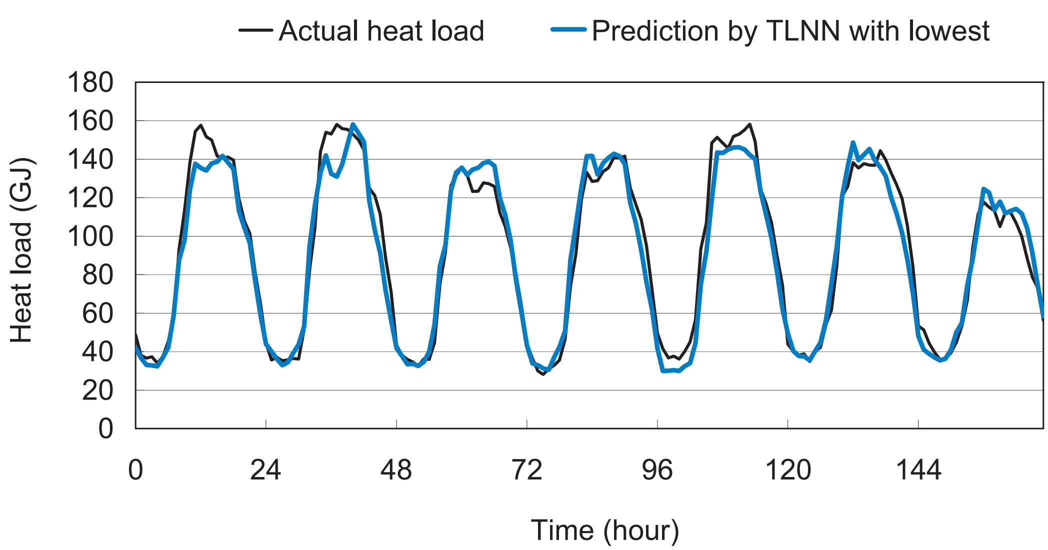

Figure 15: Prediction result by TLNN with the lowest open-air temperature for a stationary period from 2002/07/22 to 2002/07/28.

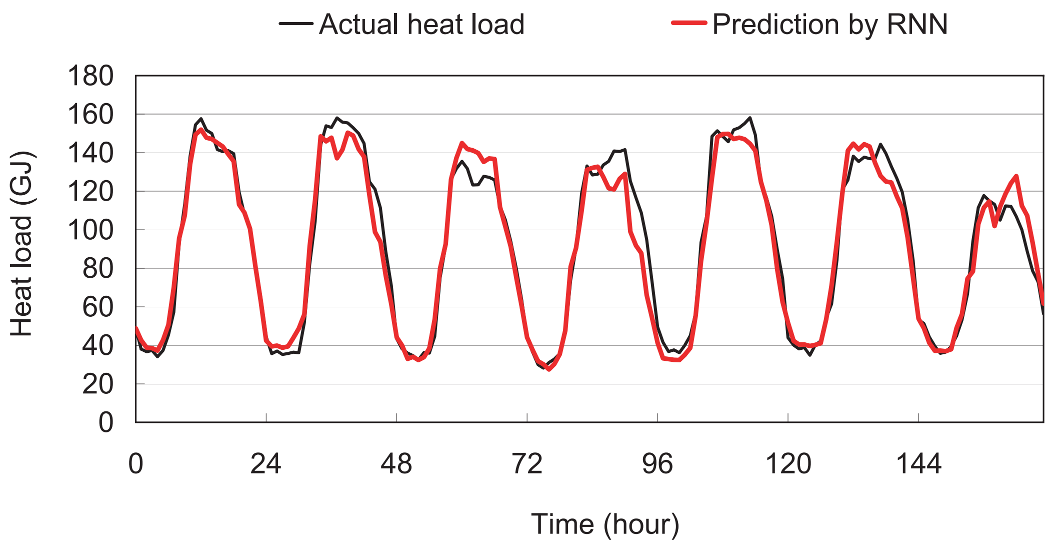

Figure 16: Prediction result by RNN for a stationary period from 2002/07/22 to 2002/07/28.

obtain better prediction than TLNN, and the proposed RNN can predict heat load with higher accuracy than TLNN and TLNN with lowest. With respect to the processing time, results (RNN: 122.2 seconds, TLNN: 72.5 seconds) are almost the same as the nonstationary period.

Furthermore, in order to check the efficiency of the proposed method for other periods, we apply TLNN and RNN into heat load prediction from February to November of 2002. Table 4 shows mean square errors and normalized root mean square errors obtained by TLNN and RNN for each month.

In each month except April (2002/04), the prediction by the proposed RNN is more accurate than that by TLNN. Particularly, the superiority of RNN to TLNN is remarkable in July, August and September when the trend in heat load is likely to be observed. On the other hand, for April, RNN is a bit inferior to TLNN. We surmise that the prediction

Table 4: Results for each month from 2002/02 to 2002/11.

	MSE (GJ^2)		PNRMSE (%)	
	TLNN	RNN	TLNN	RNN
2002/02	2.53^2	2.24^2	13.00	11.51
2002/03	4.38^2	3.54^2	17.17	13.88
2002/04	5.83^2	6.20^2	17.67	18.79
2002/05	9.60^2	8.43^2	24.00	21.08
2002/06	10.37^2	7.91^2	19.54	14.90
2002/07	16.76^2	11.44^2	17.25	11.78
2002/08	24.69^2	16.57^2	25.28	16.97
2002/09	17.20^2	12.43^2	25.97	18.76
2002/10	8.74^2	6.63^2	19.94	15.13
2002/11	3.78^2	3.55^2	15.52	14.57

by RNN becomes less accurate since heat load would extremely vary as the temperature fluctuates in April.

These experiments in this section suggest that the proposed RNN is promising as a heat load prediction method for DHC systems since its performance is generally higher than other existing methods.

6 Conclusion In the present paper, focusing on heat load prediction for DHC systems, we improved an existing heat load prediction method which is tentatively used in an actual DHC plant. For the purpose of predicting the change of heat load which is independent of the highest open-air temperature in a day, we adopt the lowest open-air temperature in a day as an input data in consideration of the characteristic of heat load data and show its significance by both the contribution ratio (CR) and Akaike's information criterion (AIC). In addition, in order to improve the prediction accuracy for periods when heat load is nonstationary, we adopt a recurrent neural network (RNN) instead of a three-layered neural network (TLNN). Furthermore, the superiority of the proposed prediction method using the lowest open-air temperature and RNN to the existing method was shown through numerical experiments using actual data in various periods.

References

[1] J.T. Connor and R.D. Martin, Recurrent neural networks and robust time series prediction, IEEE Transactions on Neural Networks, vol. 5, no. 2, pp. 240–254, March 1994.

[2] E. Dotzauer, Simple model for prediction of loads in district-heating systems, Applied Energy, vol. 73, no. 3-4, pp. 277–284, November-December 2002.

[3] R.E. Kalman, A new approach to linear filtering and prediction problems, Transactions of the ASME - Journal of Basic Engineering, vol. 82D, no. 1, pp. 35–45, March 1960.

[4] R.D. Martin and D.J. Thompson, Robust-resistant spectrum estimation, Proceedings of the IEEE, vol. 70, no. 9, pp. 1097–1115, September 1982.

[5] M. Sakawa, K. Kato, S. Ushiro and M. Inaoka, Operation planning of district heating and cooling plants using genetic algorithms for mixed integer programming, Applied Soft Computing, vol. 1, no. 2, pp. 139–150, August 2001.

[6] M. Sakawa, K. Kato, S. Ushiro, Operation planning of district heating and cooling plants through genetic algorithms for nonlinear 0-1 programming, Computers & Mathematics with Applications, vol. 42, no. 10-11, pp. 1365–1378, November-December 2001.

[7] M. Sakawa, K. Kato and S. Ushiro, Cooling load prediction in a district heating and cooling system through simplified robust filter and multi-layered neural network, Applied Artificial Intelligence, vol. 15, No. 7, pp. 995–1000, 1999.

[8] M. Sakawa, K. Kato and S. Ushiro, Operational planning of district heating and cooling plants through genetic algorithms for mixed 0-1 linear programming, European Journal of Operational Research, vol. 137, no. 3, pp.677–687, 2002.

[9] M. Sakawa, S. Ushiro, K. Kato and T. Inoue, Cooling load prediction through radial basis function network using a hybrid structural learning and simplified robust filter, Transaction of the Institute of Electronics, Information and Communication Engineers, vol. J82-A, no. 1, pp. 31–39, January 1999 (in Japanese).

[10] M. Sakawa, S. Ushiro, K. Kato and T. Inoue, Cooling load prediction through radial basis function network and simplified robust filter, Journal of Japan Society for Fuzzy Theory and Systems, vol. 11, no. 1, pp. 112–120, February 1999 (in Japanese).

[11] D.E. Rumelhart, G.E. Hinton and R.J. Williams, Learning representations by back propagating errors, Nature, Vol. 323, No. 9, pp. 533–536, 1986.

[12] R. Williams and D. Zipser, A learning algorithm for continually running fully recurrent neural networks, Neural Computation, Vol. 1, Vol. 2, pp. 270–280, 1989.

Faculty of Engineering Hiroshima University, 1-4-1, Kagamiyama, Higashi-Hiroshima, 739-8527 JAPAN

E-mail : katagiri-h@hiroshima-u.ac.jp